ISSN 1674-1056
http://cpb.iphy.ac.cn
http://iopscience.iop.org/cpb
中国物理 B
Chinese Physics
中国物理
Chinese Physics B

First-principles study on the mechanics, optical, and phonon properties of carbon chains

Jin-Ping Li(李金平), Song-He Meng(孟松鹤), Han-Tao Lu(陆汉涛), Takami Tohyama(遠山貴巳)

Citation: Chin. Phys. B . 2018, 27(11): 117101. **doi:** 10.1088/1674-1056/27/117101

Journal homepage: http://cpb.iphy.ac.cn; http://iopscience.iop.org/cpb

What follows is a list of articles you may be interested in

Effect of Mn doping on mechanical properties and electronic structure of WCoB ternary boride by first-principles calculations

Tong Zhang(张桐), Hai-Qing Yin(尹海清), Cong Zhang(张聪), Xuan-Hui Qu(曲选辉), Qing-Jun Zheng(郑清军)

Chin. Phys. B . 2018, 27(10): 107101. **doi:** 10.1088/1674-1056/27/10/107101

Multiscale energy density algorithm and application to surface structure of Ni matrix of superalloy

Min Sun(孙敏), Chong-Yu Wang(王崇愚), Ji-Ping Liu(刘吉平)

Chin. Phys. B . 2018, 27(9): 097105. **doi:** 10.1088/1674-1056/27/9/097105

Site preferences of alloying transition metal elements in Ni-based superalloy: A first-principles study

Baokun Lu(路宝坤), Chong-Yu Wang(王崇愚), Zhihui Du(都志辉)

Chin. Phys. B . 2018, 27(9): 097102. **doi:** 10.1088/1674-1056/27/9/097102

Electronic properties of defects in Weyl semimetal tantalum arsenide

Yan-Long Fu(付艳龙), Chang-Kai Li(李长楷), Zhao-Jun Zhang(张昭军), Hai-Bo Sang(桑海波), Wei Cheng(程伟), Feng-Shou Zhang(张丰收)

Chin. Phys. B . 2018, 27(9): 097101. **doi:** 10.1088/1674-1056/27/9/097101

The effects of combining alloying elements on the elastic properties of *γ*-Ni in Ni-based superalloy: High-throughput first-principles calculations

Baokun Lu(路宝坤), Chongyu Wang(王崇愚)

Chin. Phys. B . 2018, 27(7): 077104. **doi:** 10.1088/1674-1056/27/7/077104

First-principles study on the mechanics, optical, and phonon properties of carbon chains*

Jin-Ping Li(李金平)[1,†], Song-He Meng(孟松鹤)[1], Han-Tao Lu(陆汉涛)[2], and Takami Tohyama(遠山貴巳)[3]

[1] National Key Laboratory of Science and Technology on Advanced Composites in Special Environments, Center for Composite Materials and Structure, Harbin Institute of Technology, Harbin 150080, China

[2] Center for Interdisciplinary Studies & Key Laboratory for Magnetism and Magnetic Materials of the Ministry of Education, Lanzhou University, Lanzhou 730000, China

[3] Department of Applied Physics, Tokyo University of Science, Tokyo 125-8585, Japan

(Received 26 June 2018; revised manuscript received 28 August 2018; published online 24 October 2018)

Besides graphite, diamond, graphene, carbon nanotubes, and fullerenes, there is another allotrope of carbon, carbyne, existing in the form of a one-dimensional chain of carbon atoms. It has been theoretically predicted that carbyne would be stronger, stiffer, and more exotic than other materials that have been synthesized before. In this article, two kinds of carbyne, i.e., cumulene and polyyne are investigated by the first principles, where the mechanical properties, electronic structure, optical and phonon properties of the carbynes are calculated. The results on the crystal binding energy and the formation energy show that though both are difficult to be synthesized from diamond or graphite, polyyne is more stable and harder than cummulene. The tensile stiffness, bond stiffness, and Young's modulus of cumulene are 94.669 eV/Å, 90.334 GPa, and 60.62 GPa, respectively, while the corresponding values of polyyne are 94.939 eV/Å, 101.42 GPa, and 60.06 GPa. The supercell calculation shows that carbyne is most stable at $N = 5$, where N is the supercell number, which indicates that the carbon chain with 10 atoms is most stable. The calculation on the electronic band structure shows that cumulene is a conductor and polyyne is a semiconductor with a band gap of 0.37 eV. The dielectric function of carbynes varies along different directions, consistent with the one-dimensional nature of the carbon chains. In the phonon dispersion of cumulene, there are imaginary frequencies with the lowest value down to −3.817 THz, which indicates that cumulene could be unstable at room temperature and normal pressure.

Keywords: carbyne, first-principles calculation, electronic structure, physical properties

PACS: 71.15.Mb, 71.15.Nc, 73.90.+f, 78.20.Ci **DOI:** 10.1088/1674-1056/27/11/117101

1. Introduction

A new type of carbon chains, called carbyne,[1] has received considerable attention in the community of materials because of its unique mechanical and electronic properties, and potential for applications in various fields, such as in nanoelectronic or spintronic devices[2–7] and hydrogen storage.[8] The chemical structure of carbyne is a chain of carbon atoms that are linked either by alternate triple and single bonds (–C≡C–)—i.e., polyyne—or by consecutive double bonds (=C=C=)—i.e., cumulene.[9] Carbyne is something of a mystery because astronomers believe that they have detected its signature in interstellar space. Chemists, in contrast, have been bickering for decades over whether they had ever created this material on the Earth.[10] A couple of years ago, however, chemists successfully synthesized carbyne chains of up to 44 atoms long in a solution,[11] which comprises an important step towards the realistic application of the material.

The possibility of the realization of stable carbynes in laboratories stimulates considerable theoretical attention and investigations. Some interesting features of carbynes have been revealed and discussed recently from the theoretical side. For example, it was predicted that carbynes could be stronger, stiffer, and more exotic than other known materials.[12] However, to the best of our knowledge, the need of a fully systematic investigation of the physical properties of carbynes is still to be met. In this paper, by means of the first-principles calculations, we systematically study the mechanical properties, electronic structure, optical and phonon properties of two kinds of carbynes. A comparison with other results is also provided. We hope that the work will be helpful in further understanding caybyne to make good use of it in the future.

2. Computational methodology

First-principles calculations are performed with plane-wave ultrasoft pseudopotential by means of GGA with PW91 functional as implemented in the Cambridge sequential total energy package (CASTEP) code.[13] The ionic cores are represented by ultrasoft pseudopotential for C atoms. For

*Project supported by the National Natural Science Foundation of China (Grant No. 11672087), the Strategic Programs for Innovative Research (SPIRE), the Computational Materials Science Initiative (CMSI), and the Yukawa International Program for Quark-Hadron Sciences at YITP, Kyoto University, Japan.

†Corresponding author. E-mail: lijinping@hit.edu.cn

© 2018 Chinese Physical Society and IOP Publishing Ltd

C atom, the configuration is [He]$2s^2 2p^2$, where the $2s^2$ and $2p^2$ electrons are explicitly treated as valence electrons. The plane-wave cut-off energy is 380 eV, and the Brillouin-zone integration is performed over the $3\times3\times10$ grid sizes using the Monkorst–Pack method for structure optimization. This set of parameters assures the total energy convergence of 5.0×10^{-6} eV/atom, the maximum force of 0.01 eV/Å, the maximum stress of 0.02 GPa, and the maximum displacement of 5.0×10^{-4} Å.

In the following sections, we perform calculations on carbynes after or without having optimized the geometry structure by the GGA-PW91.

3. Crystal binding energy and formation energy

Crystal binding energy W is defined as the energy difference (per atom) between the total energy E_0 when the crystalline is stable for N atoms and the total energy of the N atoms E_N when they are in a free state; i.e., $W=(E_N-E_0)/N$. For covalent crystals, a larger binding energy usually means more stable structure with higher melting-point and hardness. In our case, the energy of a free carbon atom is calculated to be -147.017951 eV. For cumulene, E_N is given by the total energy of 2 free carbon atoms, while E_0 for two carbon atoms is estimated to be -308.375891 eV. Thus the crystal binding energy reads $W=[(-147.017951)\times2-(-308.375891)]/2=7.1699945$ eV. In contrast, for polyyne $E_0=-308.378995$ eV, leading to $W=7.1715465$ eV. The values of W for cumulene and polyyne are consistent with previously reported values of $W=6.99$–8.19 eV.[7] We may first conclude that both cumulene and polyyne are stable against free carbons due to positive W. Second, polyyne is more stable than cumulene with the energy gain of 1.55 meV per atom. This is consistent with the fact that the unit structure of cumulene (=C=C=) is known to undergo a Peierls transition into that of polyyne (–C≡C–).[9]

The stability of carbynes can be further examined by comparing the formation energy E_f with those of other carbon allotropes; i.e., diamond and graphite. The crystal formation energy E_f, is that the total energy of the covalent crystal, E_0, subtracts total energy of the element crystalline. The total energy of diamond and graphite for two carbon atoms are calculated to be -309.873429 eV and -310.129136 eV, respectively. We can see that they are lower than E_f for both cumulene and polyyne, which underlines the difficulty of synthesizing carbynes from diamond or graphite. The significant energy difference also indicates a possible instability of carbynes at room temperature.

4. Mechanical properties

4.1. Cumulene

4.1.1. Tensile stiffness

The most basic mechanical property of the carbyne chain is its tensile stiffness, which is defined as

$$C=\frac{1}{a}\frac{\partial^2 E}{\partial\varepsilon^2}, \tag{1}$$

where a is the unit cell length (2.565 Å), E is the strain energy per two C atoms, and ε is the strain. As shown in Fig. 1, fitting our numerical data to Eq. (1) by a second-order polynomial yields a tensile stiffness of $C=94.669$ eV/Å, which is in agreement with earlier work, $C=95.56$ eV/Å.[12]

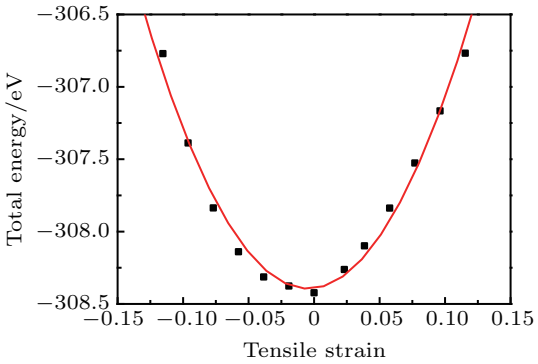


Fig. 1. (color online) The dependence of the total energy on stretch strain for cumulene. Black dots are numerical results and the red curve is fitting with second-order polynomial.

4.1.2. Bond stiffness

Another mechanical property is the bond stiffness, which describes the change of the bond length between neighboring carbon atoms (d) with respect to an applied pressure (P). Taking the bond length at ambient pressure P_0 to be d_0, we expand the relative bond length (d/d_0) up to the second order of P,

$$d/d_0=C_0+C_1P+C_2P^2. \tag{2}$$

The coefficients in Eq. (2) are determined by fitting the calculated d/d_0 to a polynomial. The chemical bond stiffness K is given by

$$K=\left|\frac{\mathrm{d}\,(d/d_0)}{\mathrm{d}P}\right|^{-1}=|C_1+2C_2P|^{-1}. \tag{3}$$

Figures 2(a) and 2(b) show the first-principles results of the hydrostatic pressure dependence of the relative bond length d/d_0 and the bulk modulus B in cumulene, respectively. The red curves are produced by a second-order polynomial fitting. In Fig. 2(a), we obtain the value of the chemical bond stiffness K for cumulene to be 90.334 GPa. In Fig. 2(b), we can observe that the bulk modulus B increases with the pressure. When P is about 1 GPa, B reaches 1531.4 GPa. The above data show that cumulene is very stiff, even among the carbon materials; e.g., the bulk modulus of diamond is about 600 GPa, and the value of cumulene is more than 1500 GPa.

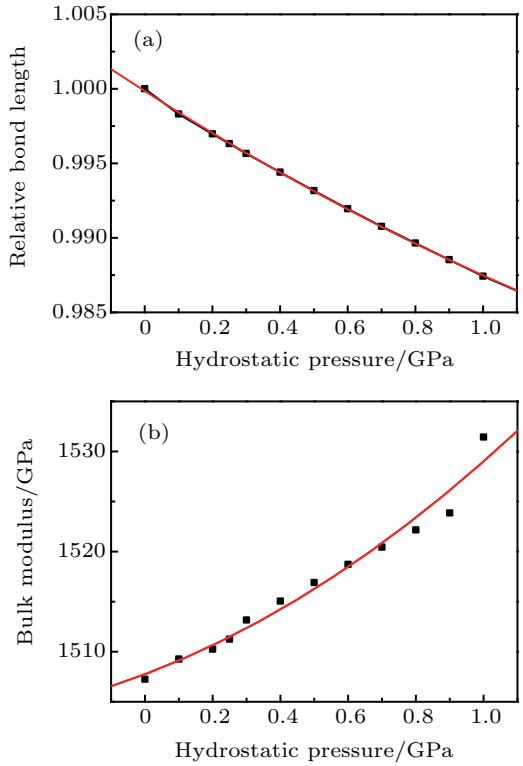


Fig. 2. (color online) (a) The relative bond length d/d_0 and (b) the bulk modules B as a function of hydrostatic pressure for cumulene.

4.1.3. The relationship between stress and strain

The relation between stress and strain in cumulene can be studied from two aspects—i.e., either by studying the response of the bond length to different loads applied to the chain (as in Fig. 3)—or by determining the consequent stress values following the change of the bond length (as in Fig. 4). It can be observed in Fig. 3 that the strain increases almost linearly with the applying stress up to 2.5 GPa, while the linearity of the decrease in the bulk modulus with the tensile stress is also plain in Fig. 3(b). From Fig. 4, the monotonic increase (though not linearly) of the tensile stress with respect to the extending of the bond length can be observed.

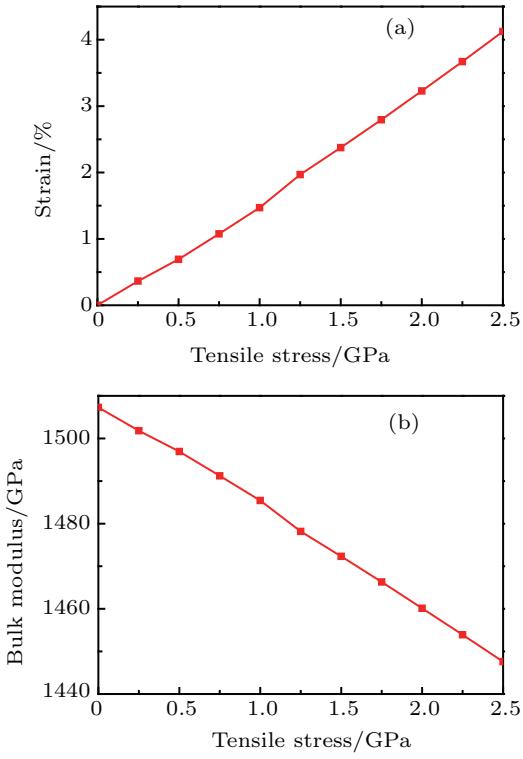


Fig. 3. (color online) (a) The strain and (b) the bulk modulus of cumulene as a function of tensile stress.

The Young's modulus of cumulene can be calculated from Fig. 3(a) as

$$E = \frac{\sigma}{\varepsilon} = \frac{2.5\ \text{GPa}}{4.124\%} = 60.62\ \text{GPa}. \tag{4}$$

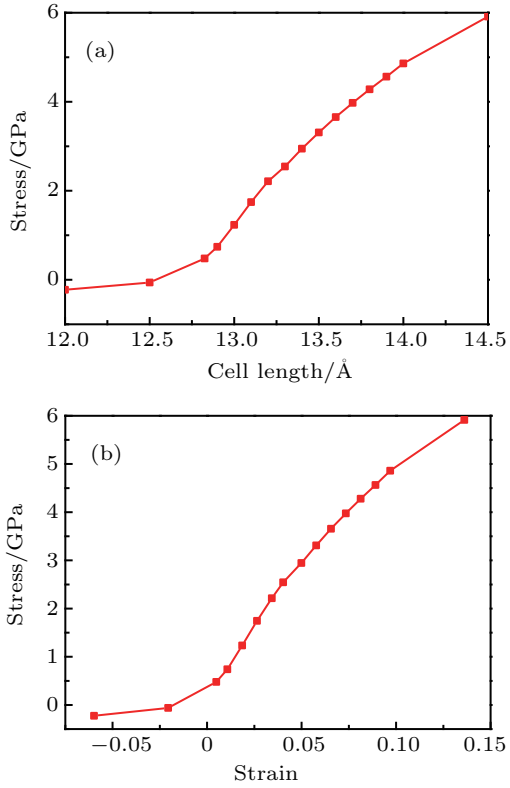


Fig. 4. (color online) The tensile stress of cumulene as a function of (a) the cell length or (b) strain.

4.2. The mechanical properties of polyyne

In this subsection, we move to the discussion of the mechanical properties of polyyne. We first calculate the tensile and bond stiffness of polyyne using the same method as in cumulene. The results for the strain dependence of the total energy and band gap are shown in Fig. 5. The tensile stiffness can be obtained from Fig. 5(a) which turns out to be 94.939 eV/Å, which coincides well with other results; e.g., 95.56 eV/Å in Ref. [12]. From Fig. 5(b), we can see that the band gap decreases with the increase of the bond strain or the bond length. We obtain the chemical bond stiffness K in polyyne to be 101.42 GPa.

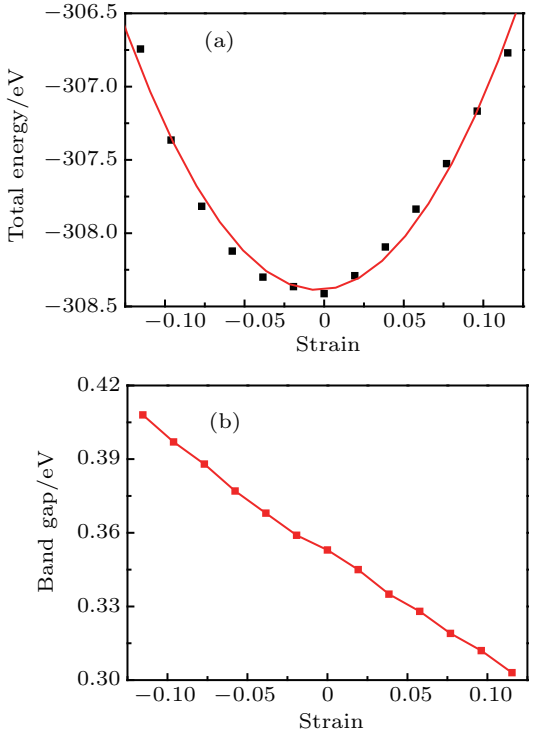


Fig. 5. (color online) (a) The total energy and (b) band gap as a function of strain.

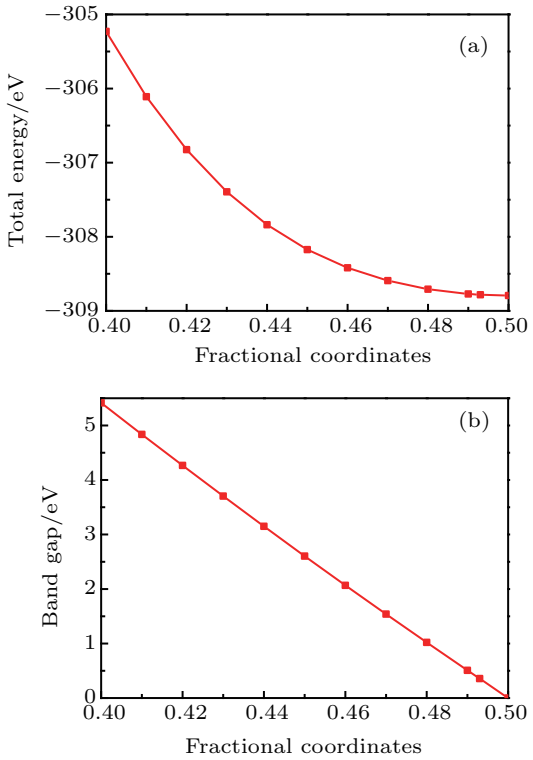


Fig. 6. (color online) (a) The total energy and (b) the band gap of polyyne as a function of the fractional coordinate without geometry optimization.

For polyyne, we are especially interested in the change of the mechanical properties with respect to the fractional coordinate of the mid-carbon atom. In the unit cell of polyyne, regarding the two fixed ends, the fractional coordinate measures the relative position of the mid-carbon atom (here the length is 0.2566 nm). In doing this, we perform the calculation without geometry optimization (otherwise with the application of geometry optimization, polyyne will automatically change into cumulene). The results of the total energy and the band gap as a function of fractional coordinate are shown in Fig. 6. We can see that both the total energy and the band gap decrease monotonically with the increase of the fractional coordinate of the mid-carbon atom from 0.40 to 0.50. Moreover, the linear dependence of the band gap on the fractional coordinate can be observed. When the fractional coordinate of the mid-carbon atom reaches 0.5—i.e., polyyne turns into cumulene—the total energy reaches its minimum value and at the same time the band gap is zero by extrapolation. We may conclude that cumulene is a conductor while polyyne is a semiconductor. From the point of view of the total energy, cumulene seems to be more stable than polyyne when the cell size is kept unchanged. However, if the cell size can be optimized, then polyyne would be more stable than cumulene, as narrated in Section 3.

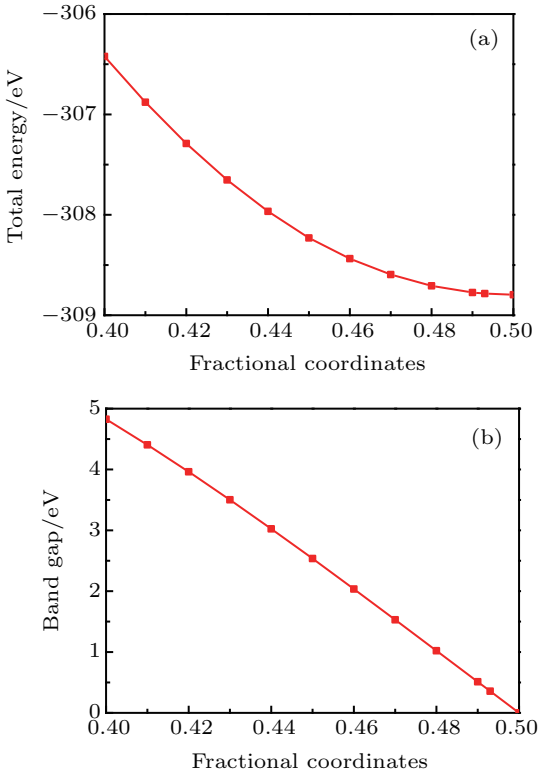


Fig. 7. (color online) (a) The total energy and (b) band gap of cumulene as a function of the fractional coordinate without geometry optimization.

A similar calculation starting from the side of cumulene without geometry optimization can also be performed. The result shows little quantitative difference compared with the case of polynne. We can see from Fig. 7 that both the total energy and the band gap decrease monotonically with the increase of the fractional coordinate of the mid-carbon atom from 0.40 to 0.50. Moreover, the linear dependence of the band gap on the

fractional coordinate can be observed. When the fractional coordinate of the mid-carbon atom is 0.4, the length between the mid-carbon atom and the end-carbon atom is 0.15396 nm, very similar to the shortest-bond length in diamond (0.1544 nm). It is well-known that diamond is a semiconductor and its band gap is 5.47 eV. When the fractional coordinate of the mid-carbon atom is 0.4, the band gap is about 5.415 eV in the polyyne, as shown in Fig. 6(b).

5. Effect of the supercell number

In this section, we discuss the impact of the adopting supercell number on the properties of polyyne and cumulene in our first-principles calculation. The results on polyyne are shown first, where the supercell number increases from $1\times1\times1$ to $1\times1\times9$. It is no surprise that the cell length linearly increases with the supercell number N (Fig. 8(a)). However, there are plain even–odd oscillations in the band gap, bulk modulus, and the final energy with respect to the change of the supercell number N (in Figs. 8(b)–8(d)). In more detail, at $N = 5$, the final energy reaches its global minimum, and at the same time the band gap and the bulk modulus reach their maximums. Meanwhile, at either $N = 4$ or $N = 6$, the situation is reversed. We may conclude that the system is most stable when the supercell number $N = 5$ in the parameter regime that we are working with.

The results for the effect of the supercell number in cumulene after geometry optimization are summarized in Fig. 9. The size of the supercell also changes from $1 \times 1 \times 1$ to $1 \times 1 \times 9$. Similar even–odd oscillations can be found. Based on the same arguments, we conclude that for cumulene, $N = 5$ is also most stable.

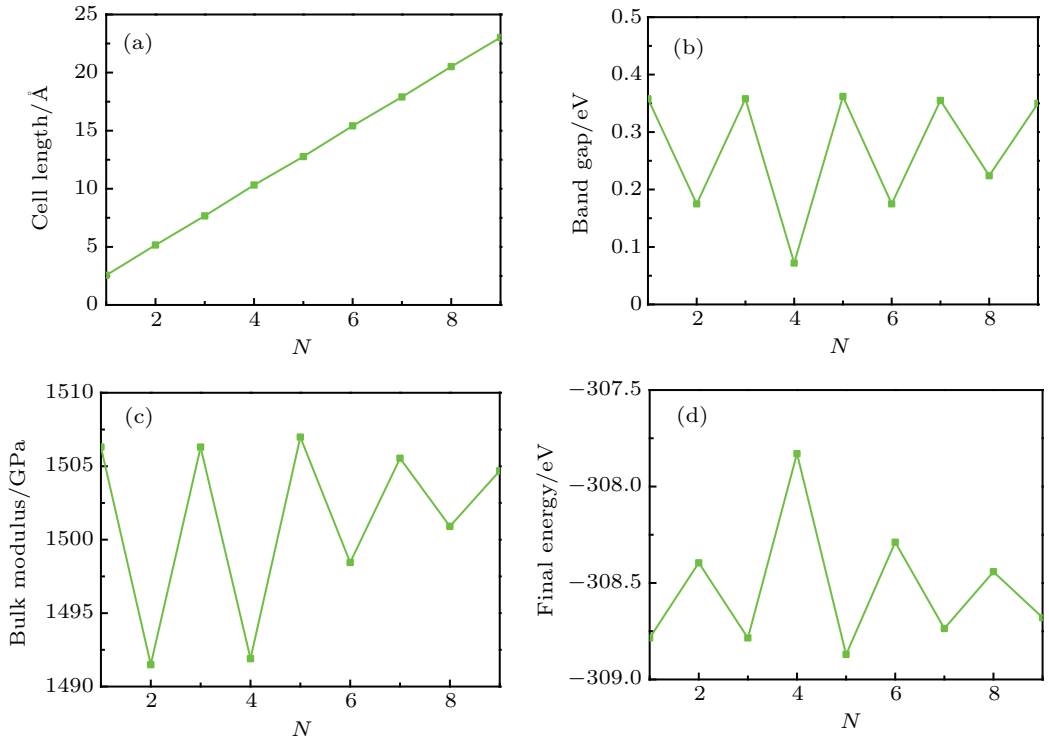


Fig. 8. (color online) (a) The cell length, (b) band gap, (c) bulk modulus, and (d) final energy in polyyne changing with the supercell number N.

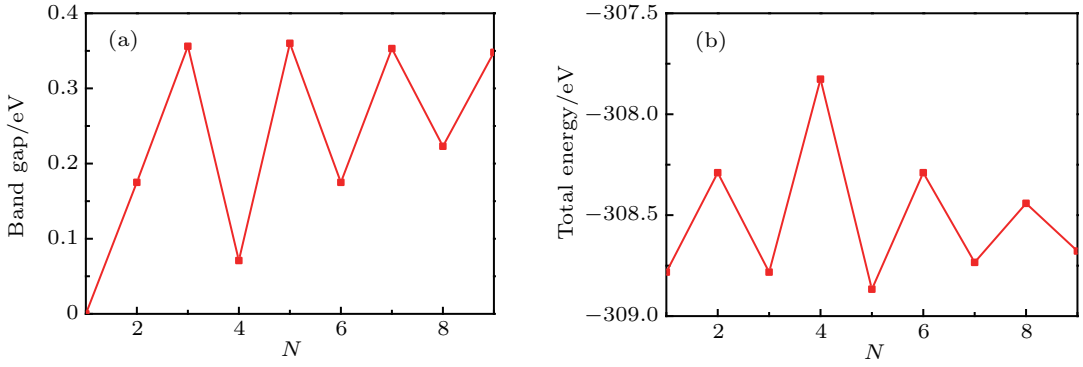


Fig. 9. (color online) The changes of (a) the band gap and (b) total energy in cumulene with the supercell number.

In the following calculation, we set the supercell of polyyne to be $1 \times 1 \times 5$ because it is the most stable configuration. We study the deformation under the unidirectional tensile stress. The calculation parameters are set as $c = 2.566 \times 5 = 12.830$ Å, GGA-PW91, ultrafine, modulus-conserving, 72 empty bands, while keeping the fractional coordinates of the mid-carbon atoms, three right angles, and a/b cell length unchanged. With the pull value (tensile stress) growing from 0 to 2.5 GPa, we obtain the band gap, bulk modulus, final energy, and strain of polyyne after geometry optimization. The results are shown in Fig. 10.

From Fig. 10, we can see that with the increase of tensile stress, the band gap (Fig. 10(a)), bulk modulus (Fig. 10(b)), and final energy (Fig. 10(c)) decrease linearly, while the strain increases (Fig. 10(d)). From Fig.10(d), we can obtain Young's modulus as 60.06 GPa for the polyyne supercell, equal to the unit cell.

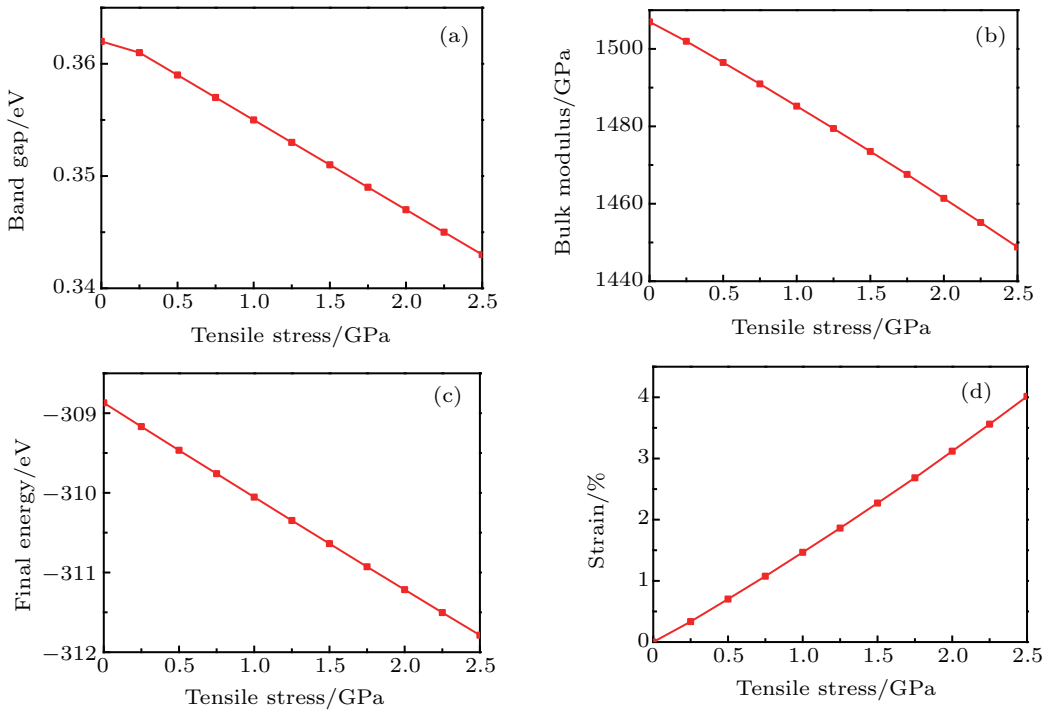


Fig. 10. (color online) (a) The band gap, (b) bulk modulus, (c) final energy, and (d) strain of polyyne changing with tensile stress.

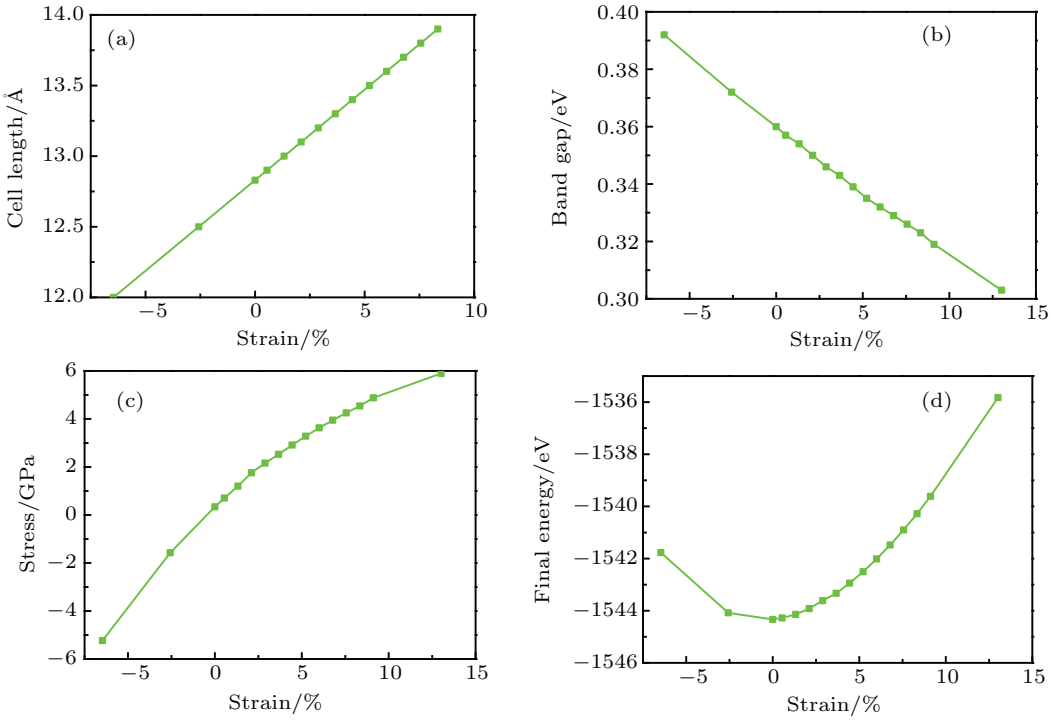


Fig. 11. (color online) (a) The cell length, (b) band gap, (c) stress, and (d) final energy of polyyne changing with strain.

Next, similar to the discussion for cumulene in Section 4.2, we study the response of polynne under the application of strain. The calculation parameters are set as $c_0 = 2.566 \times 5 = 12.830$ Å ($c = 12.770581$ Å after geometry optimization), GGA-PW91, ultrafine, modulus-conserving, 72 empty bands, and at the same time we keep the fractional coordinates of the mid-carbon atoms, three right angles, and a/b cell length unchanged. With c_0 length changed from 12 to 14 Å under the strain, we obtain the corresponding values of the cell length, band gap, stress, and final energy after geometry optimization, as shown in Fig. 11. From Figs. 11(a) and 11(b), the linear dependence of the cell length and the band gap on the strain (up to an increment of 15%) can be observed. On the other hand, the deviation from the linear dependence between stress and the applied strain is clear in Fig. 11(c). Furthermore, in Fig. 11(d) for the final energy, we can see that it is a non-monotonic function of strain and has a minimum when no strain is applied, which corresponds to $c = 12.770581$ Å after geometry optimization. It seems that we can say that the system is stable with zero applied strain.

6. Electronic structure, optical and phonon properties of cumulene

6.1. Electronic structure of cumulene

The band structure along high-symmetry points in the Brillouin zone and the density of states (DOS) are shown in Fig. 12. No band gap is observed, indicating that cumulene is a conductor. The total DOS is presented in Fig. 12(b). We can divide the valence-band regime into three parts, i.e., the lowest region between -16 eV~ -12.5 eV, the middle region of -12.5 eV~ -7.5 eV, and the upper region of -5 eV~ 0 eV, which mainly come from C 2s, C 2s+2p, and C 2p electrons, respectively.

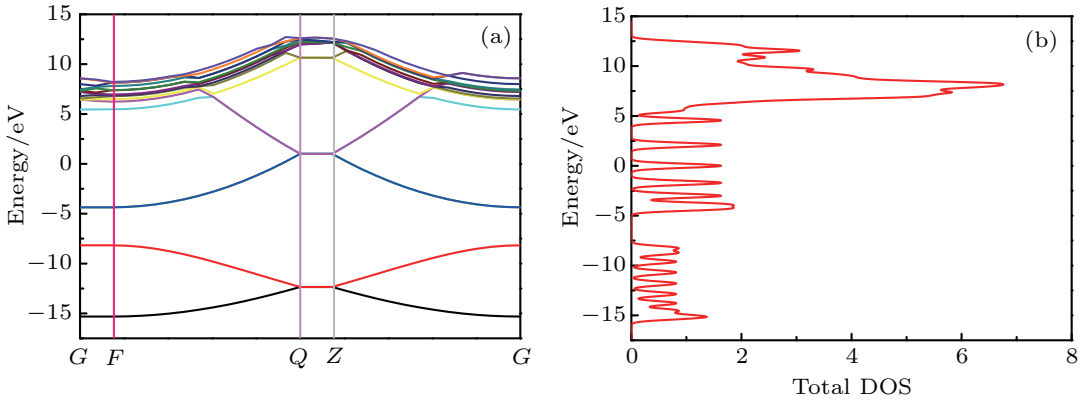


Fig. 12. (color online) (a) The band structure along high-symmetry points in the Brillouin zone and (b) the total DOS of cumulene.

6.2. Optical properties

The complex dielectric function ε contains a real part ε_1 and an imaginary part ε_2. The imaginary part ε_2, which is related to the real part of optical conductivity, can be calculated from the band structure directly by taking into account interband transitions, while the real part ε_1 can then be obtained by employing the Kramers–Kronig relations.[14] Figure 13 shows the average and the orientation dependence of the dielectric function as a function of photon energy obtained by the GGA, where (001) is the direction along the chain, and (010), (100) are transverse directions. From Fig. 13, we can determine the static dielectric constant (ε_1 at $E = 0$) of cumulene as 1.02, and the maximums of the real part and the imaginary part of the dielectric function, which are 1.155 and 0.213, appear at 9.47 eV and 9.79 eV, respectively. Moreover, the anisotropy of the dielectric function among (001), (010), and (100) is clearly observed, which is consistent with the one-dimensional nature of the carbon chains.

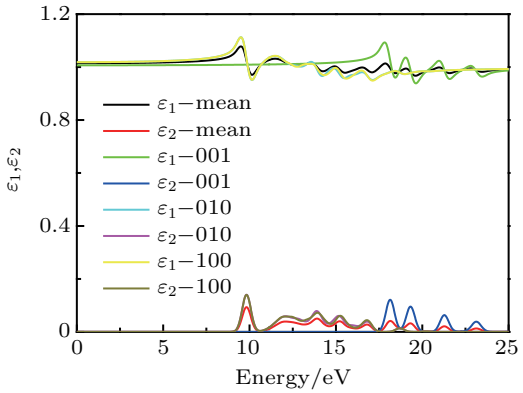


Fig. 13. (color online) The average and the orientation dependence of the complex dielectric function for cumulene.

6.3. Phonon properties

The low-energy part of the phonon dispersion of cumulene and its DOS obtained by GGA-PW91 are shown in Fig. 14. The Bradley–Cracknell notation is used for the high-symmetry points, e.g., $G = (0,0,0)$, $Q = (0.0,0.0,0.47)$, and $Z = (0.0,0.0,0.5)$. Since each unit cell of cumulene contains

two carbon atoms, there are six vibration modes (including three acoustic and three optical modes). As shown in Fig. 14, the six modes are mixed and there is no phonon band gap. If the phonon dispersion of one material has no negative frequency, then it usually means that it is kinetically stable.[15] For cumulene, there are some parts showing negative frequencies with the lowest value down to −3.817 THz, which indicates that cumulene is kinetically unstable and therefore it could be unstable at room temperature and normal pressure.

Some thermodynamic quantities obtained by GGA-PW91, including the enthalpy (which is just the summation of the Gibbs free energy and a term given by the product of temperature and entropy, T^*entropy), Gibbs free energy, entropy, and the heat capacity of the cumulene, are shown in Fig. 15. From Fig. 15(a), it can be seen that the internal energy of the cumulene rises slowly with temperature from 20 to 200 K, and then increases nearly linearly over 200 K. Entropy increases with temperature. Since the ions polarize each other when they are close to each other, the relationship line between entropy and temperature presents certain bending. The Gibbs free energy decreases with temperature concavely. With the increase of temperature, the heat capacity (shown in Fig. 15(b)) first increases fast and then slows down, gradually approaching the Dulong–Petit limit, i.e., $C = 3NkV$, in the high-temperature regime.

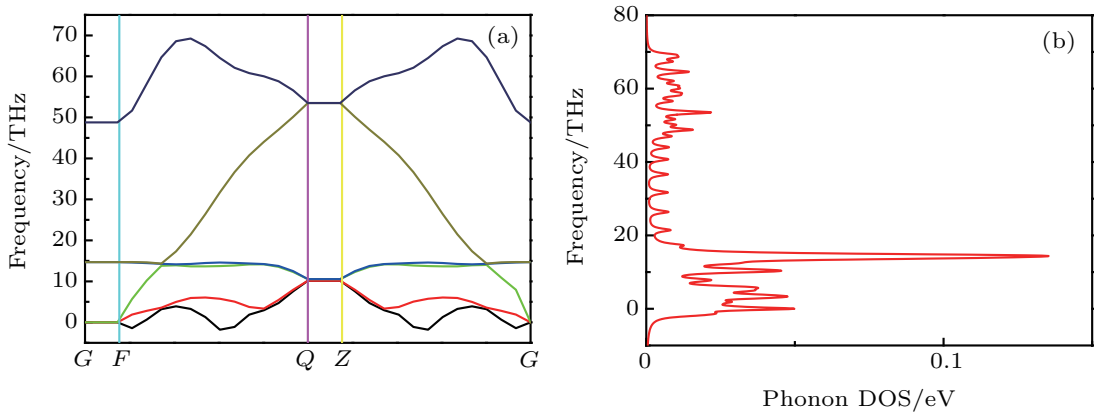


Fig. 14. (color online) (a) The low-energy part of the phonon dispersion and (b) the phonon DOS of cumulene obtained by GGA-PW91.

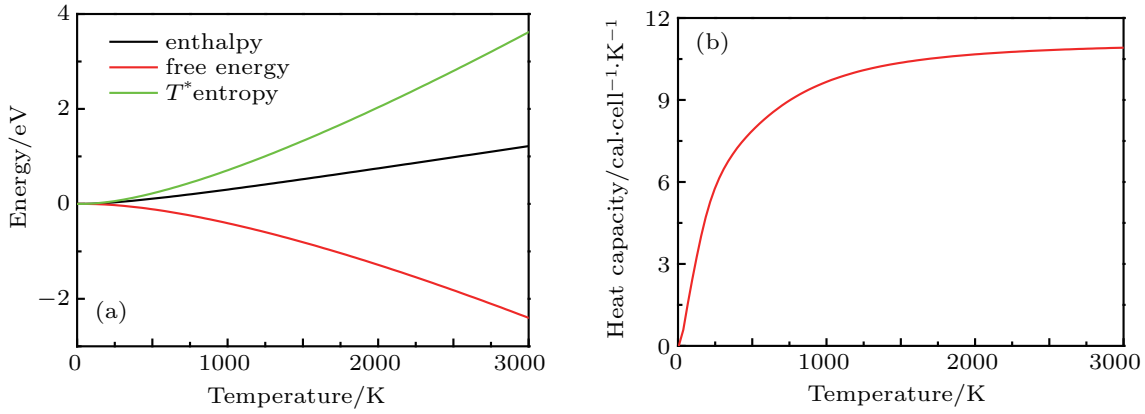


Fig. 15. (color online) (a) Some thermodynamic quantities and (b) the heat capacity of the cumulene obtained by GGA-PW (the zero point energy is 0.2599 eV).

7. Electronic structure and optical properties of Polyyne

7.1. Electronic structure

The band structure along high-symmetry points in the Brillouin zone and the DOS are shown in Fig. 16. The tiny band gap with the value of 0.37 eV is observed (Fig. 16(a)), which indicates that polyyne is a semiconductor. The gap value, different from the gapless prediction in Ref. [7], coincides with the experimental result (about 0.5 eV).[16] The total DOS is presented in Fig. 16(b). There are three parts in the valence bands; i.e., the lowest region about −20 eV∼ −15 eV, the lower region about −15 eV∼ −10 eV, and the upper region about −6 eV∼ 0 eV, which mainly come from C 2s, C 2s+2p, and C 2p electrons, respectively.

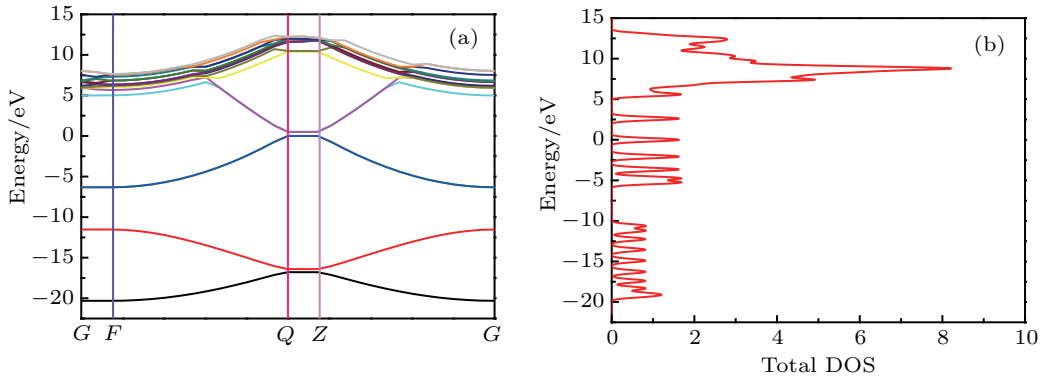


Fig. 16. (color online) (a) The band structure along high-symmetry points in the Brillouin zone and (b) the total DOS of polyyne.

7.2. Optical properties

Figure 17 shows the complex dielectric function as a function of photon energy obtained by GGA. We use three supercells—i.e., $1 \times 1 \times 1$, $1 \times 1 \times 5$, and $1 \times 1 \times 9$—for polyyene. The dielectric functions for different supercell numbers are shown in Fig. 17. We can see that with the increase of N, the dielectric function shifts toward lower energy as a whole, yet with no significant change in the shape. For $1 \times 1 \times 1$ supercell, the static dielectric constant (ε_1 at $E = 0$) is 1.03, and the maximums of the real part and the imaginary part of the dielectric function are 1.15 and 0.2, respectively. Their corresponding energy positions, around 2.5 eV, are almost identical.

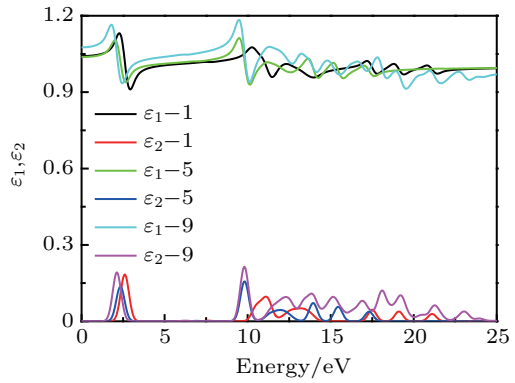


Fig. 17. (color online) The complex dielectric functions in different polyyne supercells.

8. Conclusion

We calculate the mechanical properties, electronic band structure, optical and phonon properties of the two kinds of carbyne—i.e., cumulene and polyyne—by first principles. The mechanical properties including the tensile stiffness, bond stiffness, and Young's modulus show similar behaviors, while quantitatively, polyyne turns out to be more stable and harder than cumulene. The results on the electronic band structure show that cumulene is a conductor and polyyne is a semiconductor. The supercell calculation suggests that carbyne is most stable when the supercell number $N = 5$. The dielectric function of carbynes varies in different directions, which is consistent with the one-dimensional nature of the carbon chains. The presence of the imaginary frequencies in the phonon dispersion of cumulene indicates that cumulene might be unstable at room temperature and normal pressure.

References

[1] Belenkov E A and Mavrinsky V V 2008 *Crystallogr. Rep.* **53** 83
[2] Khoo K H, Neaton J B, Son Y W, Cohen M L and Louie S G 2008 *Nano Lett.* **8** 2900
[3] Zanolli Z, Onida G and Charlier J C 2010 *ACS Nano* **4** 5174
[4] Zeng M G, Shen L, Cai Y Q, Sha Z D and Feng Y P 2010 *Appl. Phys. Lett.* **96** 042104
[5] Akdim B and Pachter R 2011 *ACS Nano* **5** 1769
[6] Artyukhov V I, Liu M and Yakobson B I 2014 *Nano Lett.* **14** 4224
[7] Zhang Y Z, Su Y J, Wang L, Kong E S, Chen X S and Zhang Y F 2011 *Nanoscale Res. Lett.* **6** 577
[8] Sorokin P B, Lee H, Antipina L Y, Singh A K and Yakobson B I 2011 *Nano Lett.* **11** 2660
[9] Cahangirov S, Topsakal M and Ciraci S 2010 *Phys. Rev. B* **82** 195444
[10] Webster A 1980 *Mon. Not. R. Astron. Soc.* **192** 7P
[11] Chalifoux W A and Tykwinski R R 2010 *Nat. Chem.* **2** 967
[12] Liu M J, Artyukhov V I, Lee H, Xu F B and Yakobson B I 2013 *ACS Nano* **7** 10075
[13] Segall M D, Lindan P J D, Probert M J, Pickard C J, Hasnip P J, Clark S J and Payne M C 2002 *J. Phys. –Condens. Mat.* **14** 2717
[14] Wang J, Li H P and Stevens R 1992 *J. Mater. Sci.* **27** 5397
[15] Zhang Q, Zhang H and Cheng X L 2018 *Chin. Phys. B* **27** 027301
[16] Kudryavtsev Y P, Evsyukov S E, Guseva M B, Babaev V G and Khvostov V V 1993 *Russ. Chem. Bull.* **42** 399